

Efficient Dispersion of Magnetite Nanoparticles in the Polyurethane Matrix Through Solution Mixing and Investigation of the Nanocomposite Properties

Mohsen Ashjari · Ali Reza Mahdavian ·
Nadereh Golshan Ebrahimi · Yasamin Mosleh

Received: 19 September 2009 / Accepted: 14 February 2010 / Published online: 3 March 2010
© Springer Science+Business Media, LLC 2010

Abstract Recent studies on inorganic/polymer nanocomposites have shown enhancements in thermal, mechanical, and chemical properties over the neat polymer without compromising density, toughness, and processibility. When nanoparticles are incorporated into the polymer matrix, significant enhancements in thermal and mechanical properties of the nanocomposite are observed. The present study is focused on the preparation and characterization of nano-size magnetite-reinforced PU composites, which induces magnetic properties to a specific thermoplastic polyurethane elastomer. The nanocomposites are prepared and the effects of magnetite content on thermal, mechanical, and magnetic properties of the nanocomposites are evaluated. Ultrasonication was used to disperse the nanoparticles and break up any large clumps and aggregates and followed by mechanical mixing. The magnetic nanocomposites were characterized by FT-IR spectroscopy, thermogravimetric analysis (TGA), scanning electron microscopy (SEM), and vibrating sample magnetometry (VSM). Characterization of the magnetic nanocomposite by FT-IR showed a successful incorporation of magnetite nanoparticles into the polymeric matrix. TGA and magnetometry of the magnetic nanocomposites revealed the amount of magnetite that was incorporated into the polymeric phase. Finally, the corresponding magnetization behavior of the nanocomposites was studied.

Keywords Thermoplastic elastomer · Nanocomposite · Polyurethane · Magnetite · Ultrasound

1 Introduction

Nanotechnology is one of the most promising areas of materials science for the development of advanced materials for engineering applications. The investigation of nanoparticles is an extremely active area since these substances may be used for their novel electronic, magnetic, optic, thermal, and catalytic properties and other technological and biological applications [1].

Nanocomposites within a matrix constitute an important class of nanostructured material and superparamagnetic nanocomposites are materials that have homogeneously dispersed superparamagnetic nanoparticles within a solid matrix. The versatility of such materials allows biomedical applications [2–6], such as magnetic separations and magnetic materials for high-frequency applications [7].

Among the different matrices that can be used to embed nanoparticles, polymers are of particular interest because of their wide range of properties. For example, shape memory polymers (SMP) are polymeric networks equipped with suitable molecular switches, which are sensitive to an external stimulus. Much attention has been paid to the possibility of inducing thermomechanical actuation in SMP by techniques other than conventional heating; e.g., illumination with infrared light [8] or application of electrical current [9]. If nano- or micro-sized magnetic particles such as magnetite (Fe_3O_4) are incorporated into SMP, inductive heating of these materials by electromagnetic fields can be used to induce the shape memory effect [10, 11].

Inorganic nanoparticles generally possess very high mechanical and thermal properties, whereas polymers are

M. Ashjari · A. R. Mahdavian (✉)
Polymer Science Department, Iran Polymer and Petrochemical
Institute, P.O. Box 14965-115, Tehran, Iran
e-mail: a.mahdavian@ippi.ac.ir

N. G. Ebrahimi · Y. Mosleh
Department of Chemical Engineering, Tarbiat Modares
University, P.O. Box 14115-111, Tehran, Iran

usually thermally and mechanically weak. Moreover, since the surface energy of nanoparticles is very high due to their dimensions, with specific care, they can be mixed with polymers at the molecular level. Depending on the level of interaction between the nanoparticles and polymer chain, one can produce a material that is mechanically superior and thermally stable. However, due to their high surface energy, nanoparticles tend to agglomerate and, in most cases, are very difficult to disperse uniformly into the polymer matrix. Agglomerated nanoparticles act as defects and can have detrimental effect on polymer performance. Thus, it is imperative to disperse the nanoparticles into the polymer matrix when they are in the liquid phase in order that interactions at the molecular level can be achieved to produce a material with better thermal and mechanical properties. When nanoparticles are dispersed uniformly into a polymer, they produce a large number of interfacial regions relative to micro-composites [12].

Thermoplastic elastomers like polyurethanes (PU) have many desirable properties including high elongation at break, high strength, good abrasion resistance and high elastic modulus compared to other elastomers. They are frequently used as aerospace, automotive, electronics, and petrochemical applications [13].

The synthesis of spherical magnetic nanoparticles needs to be improved to control particle size, surface functionalization, and environmental compatibility. The most common method for the synthesis of magnetite is by co-precipitation from a solution of Fe(III) and Fe(II) salts in the presence of a base [14]. Magnetite nanoparticles have been incorporated into complicated architectures such as polymeric gels to provide magnetic field sensitive gels [15]. These gels contain magnetic particles dispersed homogeneously and confined in a polymer network. Under a non-uniform magnetic field, these particles undergo motion, which in turn induces elongation, contraction or bending of the gels with short response time.

There are a wide variety of fabrication methods for polymers containing metal nanoparticles, including physical and chemical processes; e.g., casting of polymer solutions or solution mixing. Nanoparticles can be dispersed into the matrix by melting, solution or in situ polymerization. In all these cases, the polymer matrix phase has been used to control particle shape, size, and size distribution, which are crucial factors in determining the properties of the nanocomposite. In many cases, however, aggregation of the nanoparticles occurs during the processing [16].

Some researchers have prepared PU nanocomposites containing intercalated silicate layers and examined the corresponding morphology, thermal and mechanical properties [17, 18]. These nanocomposites exhibited improved elasticity, modulus, and high optical transparency.

In this work, we report the preparation of a novel magnetite/PU (M-PU) nanocomposite and the effect of the magnetite nanoparticles on the thermal and mechanical behavior of the modified PU. A commercial thermoplastic PU elastomer, LARIPUR[®], was used. The M-PU nanocomposite was prepared by a multi-step procedure, including addition of the magnetite nanoparticles to PU dissolved in tetrahydrofuran (THF). The major goal of the work is to minimize aggregation of the magnetite nanoparticles (inorganic phase) during the dispersion process in the PU matrix (organic phase).

2 Experimental

2.1 Materials

The raw materials used in this work are as follows: LARIPUR[®] LPR 2102-85AE, which is a thermoplastic PU elastomer (polycaprolactone) purchased from Coim, Italy. The glass transition temperature (T_g) of this polyester polyurethane is $-32\text{ }^\circ\text{C}$ and the melting point is $130\text{ }^\circ\text{C}$. The polymer has a hard segment (30%) based on 1,4-butanediol and methylene diphenyl diisocyanate and soft segment based on polycaprolactone ($M_n \approx 2000$). Iron(III) chloride hexahydrate, iron(II) chloride tetrahydrate, aqueous ammonia solution (25%), THF, and oleic acid were purchased from Merck Chemical Co. and were used without further purification.

2.2 Preparation of Modified Magnetite

In a typical procedure, $\text{FeCl}_3 \cdot 6\text{H}_2\text{O}$ (8 g, 30 mmol) and $\text{FeCl}_2 \cdot 4\text{H}_2\text{O}$ (2.9 g, 15 mmol) were dissolved in 100 mL deionized water in a four-necked flask. Aqueous NH_4OH solution was added slowly with agitation at $55\text{ }^\circ\text{C}$ under N_2 to adjust the aqueous dispersion to pH 11–12. The temperature was raised to $65\text{ }^\circ\text{C}$ and the system was then mixed for 2-h at $65\text{ }^\circ\text{C}$. The solution became black due to the formation of magnetite nanoparticles. Oleic acid was then added slowly to the dispersion. The product containing dark solid particles was rinsed with ethanol three times and allowed to stand in air for 2-days at room temperature. Finally, 3 g of oleate-coated magnetite nanoparticles (oil-base) were obtained; yield, 82.6%.

2.3 Preparation of Magnetic Polyurethane (M-PU)

The magnetic nanocomposites were prepared using a solution mixing process. Solid pellets (10 g) of Laripurs were dissolved in THF (100 mL) at ambient temperature

Table 1 Several M-PU_s prepared with different magnetite content

Sample	Magnetite content ^a (wt%)
PU	0
M-PU1	4
M-PU2	8
M-PU3	12

^a $[\text{m-Fe}_3\text{O}_4 \text{ (gr)}]/[\text{polymer (gr)}] \times 100$

and magnetically stirred for 24-h. The magnetite/THF dispersion was prepared in a separate reaction vessel. The mixture of magnetite nanoparticles and THF were subjected to ultrasonic irradiation using a high intensity ultrasonic horn (Ti-horn and 20 kHz) for 15-min at amplitude of 50% to produce a homogeneous dispersion. To avoid a temperature rise and undesired solvent evaporation during the sonication, external cooling was employed by putting the mixing beaker in a thermostatic bath ($\sim 0^\circ\text{C}$) for the entire period of the ultrasound process. The monodispersed magnetite was then mixed with the PU solution under vigorous agitation using a mechanical stirrer (500 rpm) for ~ 4 -h. The reactor was sealed to avoid untimely evaporation of THF and decreasing solvent volume. To prevent sedimentation of the magnetite nanoparticles during mixing, the reactor was placed in an ultrasonic bath at the time of mechanical mixing. Complete mixing lasted 4-h and the obtained magnetic nanocomposite was fabricated by solvent evaporation. The magnetic nanocomposite films were placed in a vacuum oven for 24-h at 45°C to remove excess THF. The dried magnetic nanocomposite films were then stored in a desiccator at room temperature prior to analysis. The detailed amounts of magnetites for a series of experiments have been listed in Table 1.

The magnetite morphology was imaged by SEM. FTIR was used to evaluate the degree of hydrogen bonding in the original PU and the M-PU nanocomposite. The viscoelastic behavior was analyzed by DMTA.

Solution mixing accompanied by ultrasonic irradiation methods were chosen to disperse nanoparticles into the polymer matrix as this method is found to be effective in producing a homogeneous dispersion of nanoparticles. A shearing process through ultrasonication was used to break up any large clumps and to evenly disperse the magnetite nanoparticles in the THF. Then the magnetite/THF dispersion was poured into the Laripur/THF solution and allowed to mix to maximize dispersion of the nanoparticles in the polymer matrix.

2.4 Equipment

Fourier-transform infrared spectroscopy was performed on the films of the original PU and M-PU nanocomposite. The spectra were collected with an Equinox 55 model

spectrometer from Bruker Corp. (Germany). TGA was performed on a Perkin Elmer Pyris 1 under N_2 from room temperature to 700°C at a heating rate of $20^\circ\text{C}/\text{min}$. The dynamic mechanical analysis (DMA) measurements were performed on a Polymer Laboratories Dynamic Mechanical Thermal Analyzer (Model MK-II) over a temperature range of 25 – 200°C (Surrey, UK). Tensile tests were carried out with a universal testing machine (Instron 6025, UK) at crosshead speeds of $5\text{ mm}/\text{min}$. The size and morphology of the samples were also investigated by SEM with a Vega-II from TESCAN Co. (Czech). Magnetic properties of the particles were determined with a vibrating-sample magnetometer (VSM); model 155, PAR (Princeton Applied Research, USA). Sonication was carried out with a Bandelin SONOREX Digital Ultrasonic Bath model DK 255P and a SONOPULS Ultrasonic homogenizer ($20\text{ kHz} \pm 500\text{ Hz}$ Ultrasonic generator) Model HF-GM 2200 (BANDELIN electronic GmbH & Co. KG, Berlin, Germany).

3 Results and Discussion

To obtain a good disperse of magnetite nanoparticles in the polymer matrix, it is necessary to select a proper solvent.

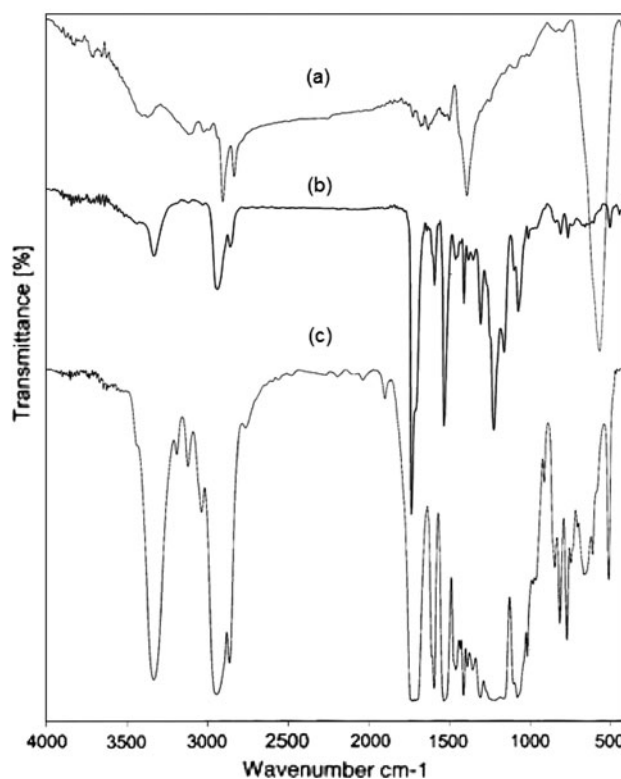


Fig. 1 The FT-IR spectra of *a* oleic acid-modified magnetite particles ($\text{m-Fe}_3\text{O}_4$), *b* original polyurethane, and *c* magnetic PU nanocomposites (M-PU)

Laripur is soluble in boiling DMF, DMAc, and THF. THF was selected because of its lower boiling point and capability of fine dispersion of oil-base magnetite nanoparticles. The dispersion process was performed with special care in order to crush magnetite agglomerates and the sedimentation process was optimized to give a minimum agglomeration of nanoparticles.

3.1 FT-IR Spectroscopy

FT-IR analysis was used to characterize the products (Fig. 1). Modified magnetites with oleic acid ($m\text{-Fe}_3\text{O}_4$) were washed with ethanol (96%) several times to remove unreacted oleic acid and excess amounts of ammonium oleate. The corresponding FT-IR spectrum of the dried powder (Fig. 1a) shows a characteristic peak of magnetite

at 570 cm^{-1} corresponding to Fe–O bending vibration. The carbonyl group of the oleic acid appears at 1709 cm^{-1} (stretching). Bands at 2854 cm^{-1} are due to C–H stretching vibration modes. This implies that oleic acid is adsorbed on the surface of Fe_3O_4 nanoparticles probably through strong hydrogen bonding and is not removed through simple washing with ethanol. The characteristic peak of magnetite (570 cm^{-1}) in the nanocomposite film appears in the M-PU2 spectrum (Fig. 1c). The FT-IR spectrum of M-PU2 shows the presence of both $m\text{-Fe}_3\text{O}_4$ and PU by comparison to the spectrum of the original PU (Fig. 1b).

3.2 Microscopic Analysis

SEM was used to investigate the morphology and size of the nanoparticles. M-PU samples were prepared by

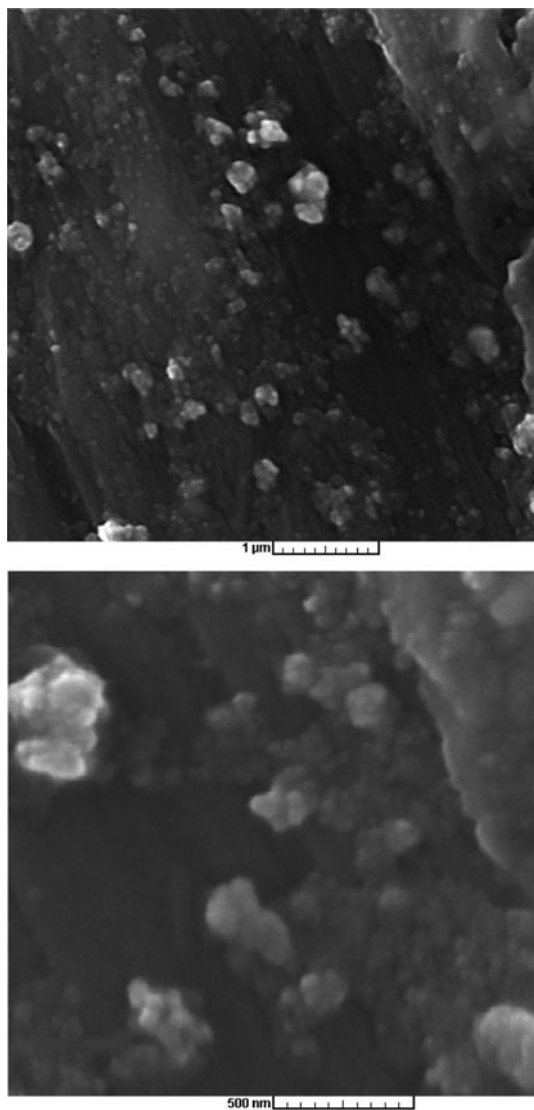


Fig. 2 SEM micrographs of the magnetite nanoparticles

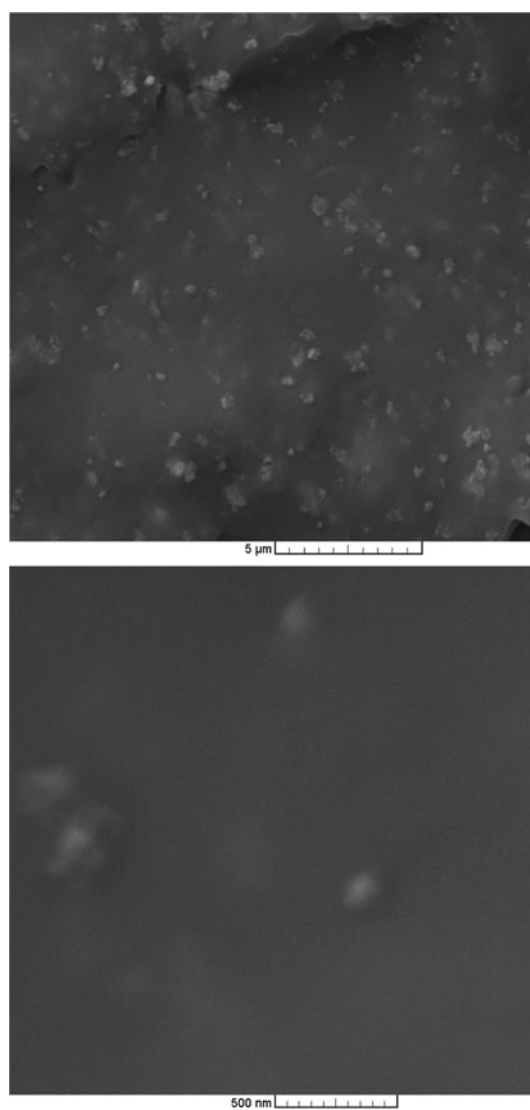


Fig. 3 SEM micrographs of the nanocomposite film from M-PU2

fracturing the samples in liquid nitrogen and scanning the cross-section. The SEM micrograph of magnetite shows the agglomerates of semi-spherical nanoparticles in which the agglomerates are about 140–160 nm (Fig. 2). After dispersion in the polymeric matrix and due to the effective dispersing procedure, the agglomerates in M-PU2 were crushed and their size was less than 100 nm (Fig. 3).

3.3 Thermal Properties

TGA thermograms were used to determine the amount of entrapped magnetite in M-PU. In the other words, they were applied to quantify the Fe₃O₄ content in the PU/Fe₃O₄ nanocomposite and also reveal the effect of magnetite on the thermal stability of M-PU. The TGA thermograms of the Fe₃O₄ nanoparticles, the original PU and the M-PU3 nanocomposite are shown in Fig. 4. The weight loss for Fe₃O₄ starts at 370 °C and is attributed to the decomposition of adsorbed oleic acid on the Fe₃O₄ surface (Fig. 4a). The maximum weight loss at 700 °C is 15 wt%, which

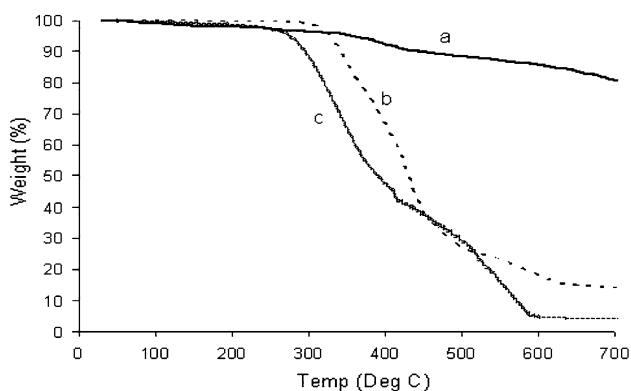
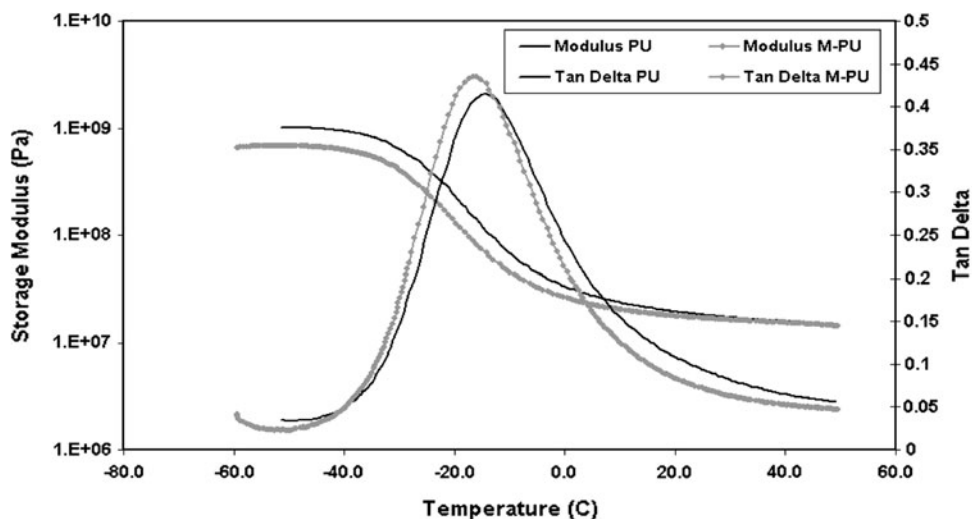


Fig. 4 TGA curves of the *a* magnetite nanoparticles (m-Fe₃O₄), *b* prepared nanocomposite film [M-PU3 sample], and *c* original PU

Fig. 5 Storage modulus and tanδ as function of temperature for the original PU and nanocomposite film (M-PU2)



indicates the relative content of adsorbed oleic acid during preparation of the modified magnetite (m-Fe₃O₄). The original PU thermally decomposes (Fig. 4c) from 300 °C and 4 wt% ash remains at 600 °C. The TGA of the corresponding magnetic nanocomposite is seen in Fig. 4b. Comparison of Fig. 4b and c indicates that M-PU3 has higher thermal stability (~60 °C higher) than PU, which is associated with the presence of magnetite nanoparticles as an additive. The difference between the residual weight percent at 700 °C for M-PU3 and the original PU indicates 15 wt% Fe₃O₄ in the modified nanocomposite.

3.4 Mechanical Properties

The viscoelastic properties of M-PU were studied by DMTA. Variation in the modulus or maximum tanδ can be attributed to several parameters as crystallization percent, crosslink density and the presence of a secondary phase between the polymeric chains. The analysis was performed on the original PU and M-PU2 (Fig. 5).

The data from DMTA graphs are listed in Table 2. The maximum storage modulus at -60 °C for M-PU2 is less than that of original PU. This suggests that resistance toward deformation in the nanocomposite decreases relative to PU; i.e., the mobility of the polymeric chains is facilitated in the presence of the dispersed nanoparticles.

Sufficient hydrogen bonding exists in PU to be responsible for physical cross-linking in the polymeric network.

Table 2 Thermal and mechanical data obtained from DMTA

Samples	T _g (°C)	Tanδ	Storage modulus (MPa)
PU	-15	0.41	1010
M-PU2	-20	0.43	735

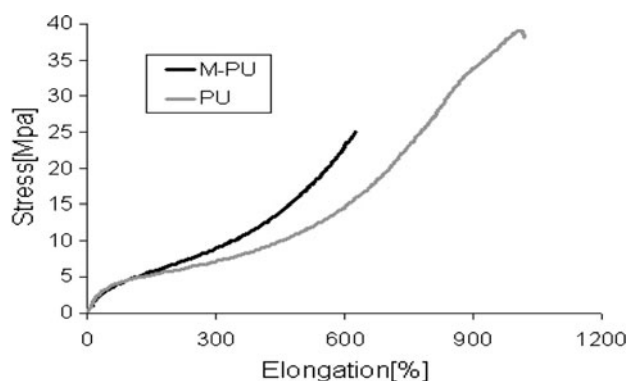


Fig. 6 Stress–strain curves of the original PU and nanocomposite film (M-PU2 sample)

The presence and finely dispersed magnetite nanoparticles between the chains can disrupt hydrogen bonding and impart more mobility to the chains. This is supported with the calculated $\tan\delta$ (Table 2), which is the ratio of loss modulus to storage modulus. As the storage modulus of the pristine PU exceed that of M-PU2, a lower value of $\tan\delta$ for PU relative to M-PU2 is predicted.

The mechanical properties of the polymeric films were also studied by tensile strength analysis. Stress–strain curves of M-PU2 and PU are given in Fig. 6. Addition of magnetite to PU does not have a specific effect on the modulus, but the variation in tensile strength at 100, 200, and 300% elongation is noteworthy (Table 3). These imply that M-PU2 during elongation has a higher tensile strength and the resulting nanocomposite will reveal more toughness and better damping properties. In other words, a larger $\tan\delta$ would be expected, which is confirmed by DMTA (Fig. 5).

The decrease in tensile strength and elongation at break for M-PU2 relative to PU is due to weak adhesion between PU and the magnetite and the decrease in the polymeric content of the test samples [19].

3.5 Magnetometry Analysis

The variation of magnetization of the polymeric nanocomposite with the applied magnetic field was recorded. Figure 7 shows the hysteresis loops of the magnetite nanoparticles modified with oleic acid ($m\text{-Fe}_3\text{O}_4$, Fig. 7a) and the magnetic nanocomposite film (M-PU2, Fig. 7b) at room temperature. Both curves are similar and S-shaped.

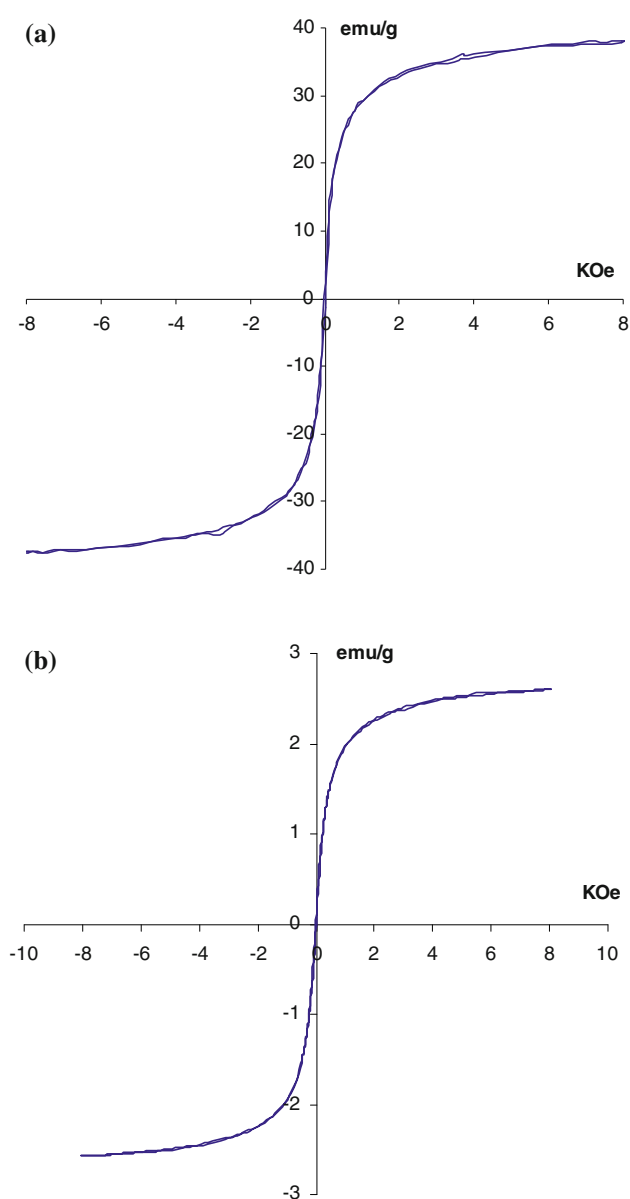


Fig. 7 Hysteresis loops by VSM of the **a** magnetite nanoparticles modified with oleic acid ($m\text{-Fe}_3\text{O}_4$) and **b** magnetic nanocomposite film (M-PU2)

The magnetic parameters are given in Table 4. The synthesized magnetite displays superparamagnetic behavior as evidenced by low coercivity (H_c) and remanence (M_r) on the magnetization loop. The corresponding

Table 3 Tensile strength test results of the samples

Samples	Tensile strength (MPa)	Elongation at tensile strength (%)	Stress at break (MPa)	Elongation at break (%)	Stress at 100% (MPa)	Stress at 200% (MPa)	Stress at 300% (MPa)
PU	38	990	33	1020	4.7	5.8	7.1
M-PU2	24	530	21	620	4.8	7.5	10.8

Table 4 Magnetic parameters of m-Fe₃O₄ and nanocomposite film (M-PU2)^a

Sample	H_c (Oe)	M_r (emu/g)	M_s (emu/g)
m-Fe ₃ O ₄	12.6 ± 0.88	0.0721 ± 0.005	38 ± 1.5
M-PU2	15.25 ± 1.01	1.7435 ± 0.009	2.6 ± 0.12

^a Errors are based on standard deviation

saturation magnetization (M_s) for m-Fe₃O₄ and M-PU2 are 38 and 2.6 emu/g, respectively.

The amount of magnetite in the synthesized M-PU2 is 7 wt% and is confirmed by the M_s ratio of m-Fe₃O₄:M-PU2; i.e., 6.8%. This also confirms that the entrapment of magnetite in the PU matrix progressed to about 95% efficiency.

4 Conclusions

Preparation of M-PU nanocomposite was achieved by a solution mixing process of magnetite nanoparticles in the presence of commercial polyurethane (Laripur[®]) in THF. The solution mixing process was performed by minimizing magnetite aggregation. SEM investigation showed that the magnetite nanoparticles were homogeneously dispersed in the PU matrix after THF casting. FTIR analysis showed the presence of magnetite nanoparticles in the polyurethane matrix. DMTA analysis showed that the presence of the magnetite nanophase affected T_g and the relaxation process of the polyurethane soft segment. TGA analysis confirmed the extent of incorporation of magnetite in the produced nanocomposite. Mechanical properties measurements revealed the presence of magnetite in M-PU and its effect on the toughness of the resulting material. VSM analyses were performed to follow the magnetic behavior of the nanocomposite and indicated superparamagnetism in the system.

Acknowledgments We wish to express our gratitude to Iran National Science Foundation (INSF) for financial support of this work (Grant # 85076/27). Also helpful assistance of Iran Polymer & Petrochemical Institute (IPPI) is greatly acknowledged.

References

1. D.I. Gittins, D. Bethell, D.J. Schiffrin, R.J. Nichols, *Nature* **408**, 67–69 (2000)
2. U. Häfeli, W. Schüt, J. Teller, M. Zborowski, *Scientific and Clinical Applications of Magnetic Carriers* (Plenum, New York, 1997)
3. Q.A. Pankhurst, J. Connolly, S.K. Jones, J. Dobson, *J. Phys. D Appl. Phys.* **36**, R167–R181 (2003)
4. A.K. Gupta, M. Gupta, *Biomaterials* **26**, 3995–4021 (2004)
5. L.P. Ramírez, K. Landfester, *Macromol. Chem. Phys.* **204**, 22–31 (2003)
6. R.A. Wassel, B. Grady, R.D. Kopke, K.J. Dormer, *Colloids Surf. A Physicochem. Eng. Aspects* **292**, 125–130 (2007)
7. C.H. Peng, C.C.H. Wang, J. Wan, J.S. Tsai, S.Y. Chen, *Mater. Sci. Eng. B Solid* **117**, 27–36 (2005)
8. D.J. Maitland, M.F. Metzger, D. Schumann, A. Lee, T.S. Wilson, *Laser Surg. Med.* **30**, 1–11 (2002)
9. J.W. Cho, J.W. Kim, Y.C. Jung, N.C. Goo, *Macromol. Rapid Commun.* **26**, 412–416 (2005)
10. R. Mohr, K. Kratz, T. Weigel, M. Lucka-Gabor, M. Moneke, A. Lendlein, *PNAS* **103**, 3540–3545 (2006)
11. M.Y. Razaq, M. Anhalt, L. Frommann, B. Weidenfeller, *Mater. Sci. Eng. A* **444**, 227–235 (2007)
12. M.C. Saha, Md.E. Kabir, S. Jeelani, *Mater. Sci. Eng. A* **479**, 213–222 (2008)
13. L.N. Philips, D.B. Valentine Parker, *Polyurethanes: Chemistry, Technology and Properties* (Ilfie Books Ltd., London, 1964)
14. S.E. Khalafalla, G.W. Reimers, *IEEE Trans. Magn.* **16**, 178–183 (1980)
15. T. Narita, A. Knaebel, J.P. Munch, S.J. Candau, M. Zrinyi, *Macromolecules* **36**, 2985–2989 (2003)
16. M.S. Kunz, K.R. Shull, A.J. Kellock, *J. Colloid Interface Sci.* **156**, 240–249 (1993)
17. B.K. Kim, J.W. Seo, H.M. Jeong, *Eur. Polym. J.* **39**, 85–91 (2003)
18. S. Zhou, L. Wu, J. Sun, W. Shen, *Prog. Org. Coat.* **45**, 33–42 (2002)
19. L.E. Nielsen, R.F. Landel, *Mechanical Properties of Polymer and Composite* (Marcel Dekker, Inc., New York, 1994)